Josephson Current in Carbon Nanotubes with Spin-Orbit Interaction

Jong Soo Lim,[1] Rosa López,[1,2] and Ramón Aguado[3]

[1]*Departament de Física, Universitat de les Illes Balears, E-07122 Palma de Mallorca, Spain*
[2]*Institut de Física Interdisciplinar i de Sistemes Complexos IFISC (CSIC-UIB), E-07122 Palma de Mallorca, Spain*
[3]*Instituto de Ciencia de Materiales de Madrid (ICMM-CSIC), Cantoblanco, 28049 Madrid, Spain*

(Received 10 May 2011; published 1 November 2011)

We demonstrate that curvature-induced spin-orbit coupling induces a 0-π transition in the Josephson current through a carbon nanotube quantum dot coupled to superconducting leads. In the noninteracting regime, the transition can be tuned by applying a parallel magnetic field near the critical field where orbital states become degenerate. Moreover, the interplay between charging and spin-orbit effects in the Coulomb blockade and cotunneling regimes leads to a rich phase diagram with well-defined (analytical) boundaries in parameter space. Finally, the 0 phase always prevails in the Kondo regime. Our calculations are relevant in view of recent experimental advances in transport through ultraclean carbon nanotubes.

DOI: 10.1103/PhysRevLett.107.196801 PACS numbers: 73.63.Fg, 71.70.Ej, 73.63.Kv, 74.45.+c

The spectrum of quantum dots (QDs) defined in carbon nanotubes (NTs) is fourfold degenerate owing to spin and valley symmetry. Recently, Kuemmeth *et al.* [1] have demonstrated that the spin and valley degrees of freedom are coupled in NTs. This spin-orbit (SO) coupling breaks the fourfold degeneracy into two Kramers doublets (time-reversed electron pairs). From a different perspective, NTs are interesting because they can support supercurrents when coupled to superconductors [2–5]. These supercurrents mainly result from resonant transmission through discrete states confined to the QD, the so-called Andreev bound states (ABS) corresponding to entangled time-reversed electron-hole Kramers pairs [6]. As both phenomena, SO and ABS, are related to time-reversed Kramers pairs, it is thus interesting to raise the following question: How are the ABS, and therefore the Josephson effect, affected by SO coupling in NTs? Here we address this question. Using various theoretical approaches we analyze this problem in all relevant transport regimes and demonstrate that the SO coupling is able to reverse the supercurrent, namely, to induce a 0 to π transition, even in the noninteracting regime.

The valley isospin ($\tau = \pm$) originates from the two equivalent dispersion cones (K and K') in graphene, arising from time-inversion symmetry. When graphene is wrapped into a cylinder to create a NT, the valley degeneracy leads to two degenerate clockwise and counterclockwise electron orbits which encircle the NT. This degeneracy, together with spin ($\sigma = \uparrow, \downarrow$), manifests in a fourfold shell structure in the Coulomb blockade regime [7,8], as well as in a SU(4) Kondo effect in the strongly correlated regime [9,10]. Furthermore, magnetic moments associated with these orbital persistent currents are remarkably large [11], which allows one to perform detailed transport spectroscopy when an external magnetic field $B_{\parallel}$ is applied parallel to the NT axis [9,11,12]. The orbital motion of electrons also couples to a curvature-induced radial electric field. This creates an effective axial magnetic field B_{SO} which polarizes the spins along the NT axis and favors parallel alignment of the spin and orbital magnetic momenta $(K, \uparrow)$ and $(K', \downarrow)$ or antiparallel $(K, \downarrow)$ and $(K', \uparrow)$ depending on the sign of the SO coupling. As a result, the fourfold degeneracy breaks into two Kramers doublets (time-reversed electron pairs) separated by an energy Δ_{SO}

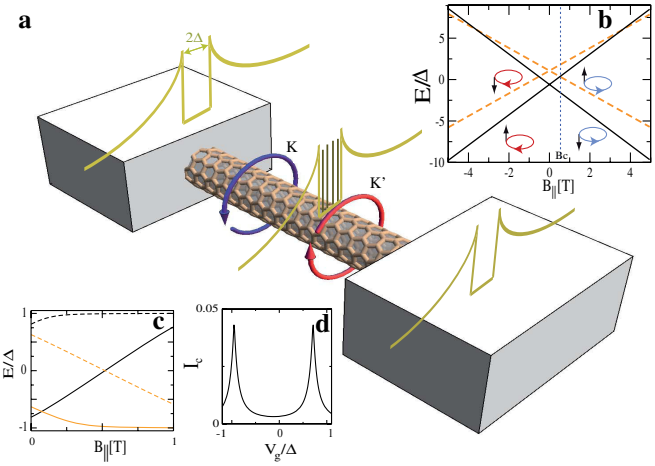

FIG. 1 (color online). Carbon nanotube coupled to superconducting leads. (a) Schematics of the system. In the QD region, discrete Andreev levels form inside the BCS gap. The figure also show the K and K' orbits encircling the NT. (b) Energy spectrum of a NT QD for realistic experimental parameters [16]. All energies are given in units of the BCS gap $\Delta = 0.25$ meV, such that $\Delta_{\mathrm{SO}}/\Delta \approx 1.66$, and referred to E_F which we take as the energy at which $(K, \uparrow)$ and $(K', \uparrow)$ cross at $B_c \approx 0.52$ T (dashed vertical line). (c) Andreev bound states corresponding to the spectrum in (b). Black and gray (orange) lines correspond to ABS calculated from the lowest and highest Kramers doublet (each contributes with two—solid and dashed lines—ABS). (d) Critical current (units $2e\Delta/\hbar$) versus gate voltage V_g. The two peaks correspond to resonant Cooper pair tunneling through SO-split Kramers pairs.

[13]. Recent experiments [14] have shown this SO effect also appears in disordered NTs in the multielectron regime.

The system we have in mind is shown in Fig. 1(a). A QD NT with SO coupling is connected to superconducting leads with a BCS density of states and superconducting phase difference ϕ. Owing to the superconducting pairing, electrons in the NT with energies below the superconducting gap (Δ) are reflected as their time-reversed particle, a hole with opposite spin and momentum. This process, known as Andreev reflection, leads to discrete states inside the gap, namely, the ABS corresponding to entangled time-reversed electron-hole Kramers pairs. We model this system by an Anderson Hamiltonian with s-wave superconducting reservoirs and with QD levels $\varepsilon_{\tau,\sigma}$ obtained from a full NT model including quantization in the longitudinal and perpendicular direction (due to QD confinement [15] and the finite diameter of the NT) and the SO coupling. The levels can be approximated as $\varepsilon_{\tau,\sigma} = \varepsilon_0 + \sigma\tau\Delta_{\mathrm{SO}} + \sigma\Delta_Z + \tau\Delta_{\mathrm{orb}}$, with $\Delta_Z = \mu_s B_\parallel$ and $\Delta_{\mathrm{orb}} = \mu_{\mathrm{orb}} B_\parallel$ (μ_s and μ_{orb} are the spin and orbital magnetic momenta [11]). The gate voltage V_g is included as a level shift in the QD spectrum (quantized level ε_0). An example of the spectrum is shown in Fig. 1(b). Interaction effects are included by using a standard Coulomb blockade model with charging energy U. Green's functions in Nambu representation are used to obtain the ABS and the two contributions to the Josephson current $I_J = I_J^{\mathrm{dis}} + I_J^{\mathrm{con}}$ of this model (full details are given in the Supplemental Materials [16]). The discrete part I_J^{dis} is due to Cooper pair tunneling through the ABS and can be written as $I_J^{\mathrm{dis}} = \frac{2e}{\hbar}\sum_{E_{1(2)}} f(E_{1(2)})\frac{\partial E_{1(2)}}{\partial\phi}$, with $f(E)$ the Fermi-Dirac function, namely, the derivative with respect to the phase of the *occupied* ABS. In the noninteracting case $U = 0$, the ABS can be obtained from

$$\left(E_{1(2)} - \varepsilon_{\mp\uparrow} + \frac{\Gamma E_{1(2)}}{\sqrt{\Delta^2 - E_{1(2)}^2}}\right) \times \left(E_{1(2)} + \varepsilon_{\pm\downarrow} + \frac{\Gamma E_{1(2)}}{\sqrt{\Delta^2 - E_{1(2)}^2}}\right) - \frac{\Gamma^2\Delta^2\cos^2(\phi/2)}{\Delta^2 - E_{1(2)}^2} = 0, \tag{1}$$

where Γ is the tunneling rate. The notation $E_{1(2)}$ indicates whether the Kramers doublet which contributes to the ABS is the ground (excited) state at $B_\parallel = 0$ [Fig. 1(b)]. Importantly, each Kramers doublet gives two solutions in Eq. (1), so in general we obtain four ABS. The two outer (inner) solutions correspond to $E_{1(2)}$ [Fig. 1(c)]. The continuous part I_J^{con} is due to particle-hole excitations for energies larger than Δ.

The results for the Josephson current are shown in Figs. 2(a) and 2(b), where a 0-π transition occurs for $B_\parallel \gtrsim B_c$, where B_c is the field at which $(K,\uparrow)$ and $(K',\uparrow)$ cross, namely, $2\mu_{\mathrm{orb}}B_c = \Delta_{\mathrm{SO}}$ [17]. The transition can be understood by studying the ABS spectrum as a function of ϕ for different $B_\parallel$ [Fig. 2(c)]. When $B_\parallel \gtrsim B_c$, the two inner ABS cross at $E_F = 0$. Owing to this, the occupied ABS for $B_\parallel \gtrsim B_c$ belong to the *same* Kramers doublet [the one formed by $(K,\uparrow)$ and $(K',\downarrow)$, which are, of course, no longer degenerate]. Importantly, they carry supercurrents of *opposite* sign which leads to a negligible I_{dis}. The main contribution is thus given by the continuum part. This continuum current can be understood as resulting from the breakdown of left and right symmetry between moving quasiparticles owing to the superconducting phase (the physical mechanism for these finite currents being analogous to persistent currents flowing in normal metal rings in the presence of a magnetic flux). Remarkably, this continuum current tends to flow opposite to the one carried by ABS, which results in π behavior [18]. It is important to note that the Josephson current may have extra magnetic-field dependences due to pair breaking in the superconducting leads (not included here). Nevertheless, it can be shown [19] that for $\Gamma/\Delta \ll 1$, which is the relevant case for our calculations, the ABS spectrum is little affected by pair breaking. In the opposite limit $\Gamma/\Delta \gg 1$, the ABS are strongly reduced and the Josephson current is mainly given by the continuum part. Thus, we expect that the 0-π transition discussed here is robust against pair-breaking mechanisms.

In Fig. 2(d), we plot the ABS as a function of gate voltage and different $B_\parallel$. At $B_\parallel = 0$, the SO-split ABS show a diamondlike shape. As $B_\parallel$ increases, the diamond closes, and, ultimately, the two inner ABS become degenerate when $B_\parallel = B_c$. When $B_\parallel \gtrsim B_c$, the ABS cross at E_F. After the crossing, the occupied ABS belong to the same Kramers doublet for a large range of $|V_g| < \Delta$ resulting in a π transition which is robust as the gate voltage is varied [Figs. 2(e) and 2(f)]. Interestingly, one can draw an analogy between SO-split Kramers pairs in our problem and spin-split ABS in standard QDs [20,21] with the role of Coulomb blockade (responsible for a finite exchange between spins in standard QDs) being played here by SO (effective exchange between Kramers doublets). Note that, without SO, the QD levels are degenerate only at $B_\parallel = 0$. In this case, the system is unpolarized in both spin and valley sectors and always remains in the 0 phase [22]. Thus, the main condition to observe the π state is to have a value of Δ_{SO} such that one has well-defined polarization between Kramers pairs. Assuming that disorder is much smaller than SO effects, this implies $\Delta_{\mathrm{SO}} \gg \Gamma$, in order to have well resolved SO levels.

We include the effect of Coulomb blockade, $U \neq 0$, by first considering the large gap limit, i.e., $\Delta \to \infty$, where the problem can be mapped onto an effective low-energy model with a superconducting pair potential due to the proximity effect $\Delta_D = \Gamma\cos(\phi/2)$. Direct diagonalization produces results for the ground state energy $E_{\mathrm{GS}}(\phi)$ and trivially $I_J = I_J^{\mathrm{dis}}$. The total spin S and the valley isospin T

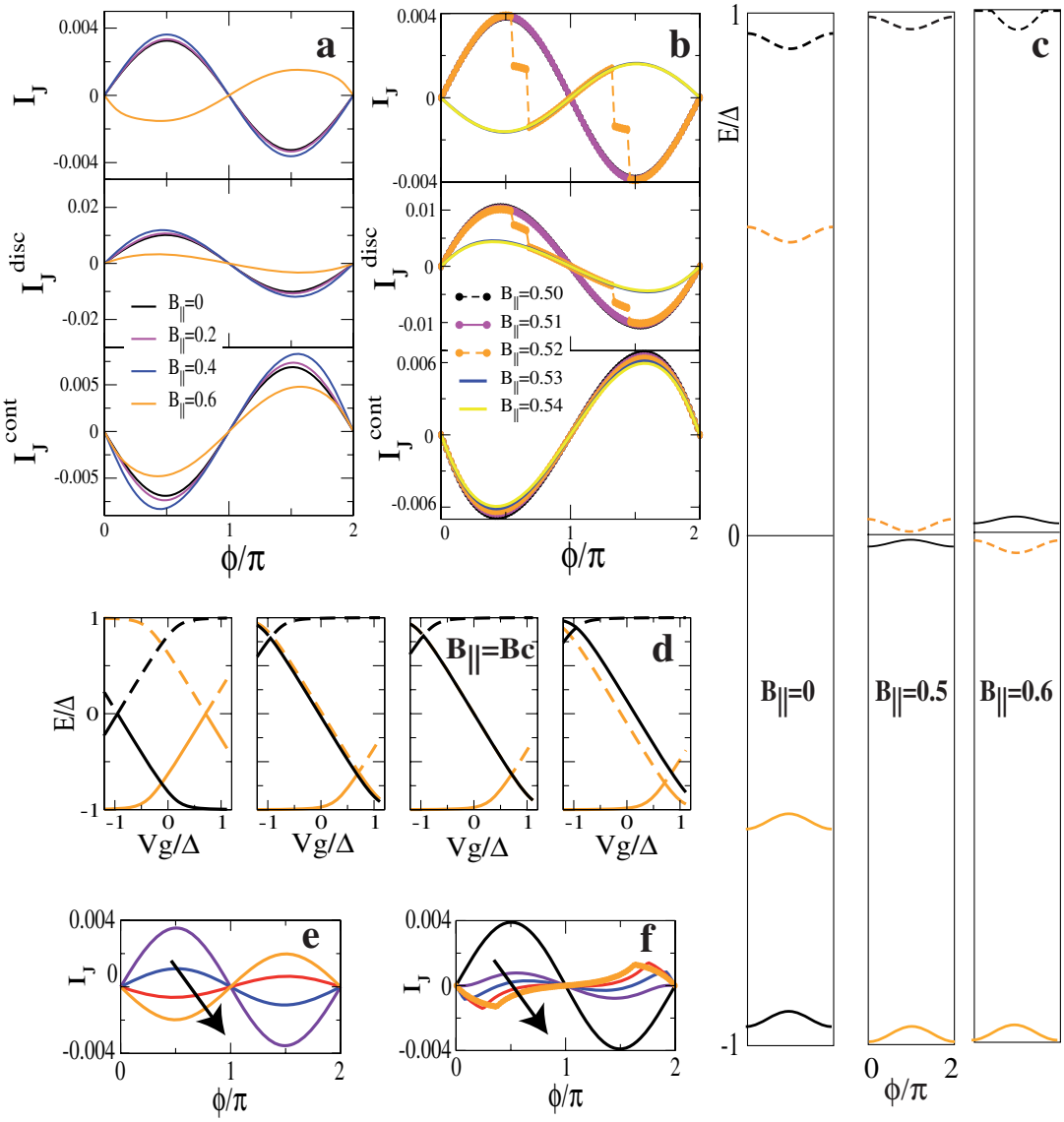

FIG. 2 (color online). SO-mediated supercurrent reversal. (a) Total (top), discrete (middle), and continuous (bottom) Josephson current (units $2e\Delta/\hbar$) as a function of phase and different $B_\parallel$ (in Tesla) for $\Gamma = 0.1\Delta$. At the highest magnetic field the system has π-junction behavior. (b) The same as (a) near the 0-π transition at $B_\parallel = B_c = 0.52$ T. (c) ABS vs ϕ for different $B_\parallel$. When $B_\parallel \gtrsim B_c$, the two inner ABS cross at $E_F = 0$ resulting in π behavior. (d) ABS versus V_g for different $B_\parallel = 0$, 0.5, 0.52, and 0.6 T, from left to right. At $B_\parallel = B_c$ the two inner ABS are degenerate for all $|V_g| < \Delta$. The π transition is robust as V_g is varied (direction of the arrow) either above (e) or below (f) $V_g = 0$.

are no good quantum numbers. Instead, $\mathcal{H}_D$ has a block diagonal form using the total projections (S_z, T_z) as a basis. For $\phi = \pi$, we find the analytical solution

$$E_{\mathrm{GS}}(\phi = \pi) = \begin{cases} V_g - \frac{1}{2}\Delta_{\mathrm{SO}} & \text{for } U > -V_g + \frac{1}{2}\Delta_{\mathrm{SO}},\ (S_z, T_z) = (\pm 1/2, \mp 1/2) \\ 2V_g - \Delta_{\mathrm{SO}} + U & \text{for } -\frac{1}{2}V_g - \frac{1}{4}\Delta_{\mathrm{SO}} < U < -V_g + \frac{1}{2}\Delta_{\mathrm{SO}},\ (S_z, T_z) = (0,0), (1,0), (0,1) \\ V_g - \frac{1}{2}\Delta_{\mathrm{SO}} + 3U & \text{for } -\frac{1}{3}V_g - \frac{1}{6}\Delta_{\mathrm{SO}} < U < -\frac{1}{2}V_g - \frac{1}{4}\Delta_{\mathrm{SO}},\ (S_z, T_z) = (\pm 1/2, \pm 1/2) \\ 4V_g + 6U & \text{for } U < -\frac{1}{3}V_g - \frac{1}{6}\Delta_{\mathrm{SO}},\ (S_z, T_z) = (0,0). \end{cases} \quad (2)$$

The ground state for arbitrary ϕ has to be calculated numerically [Fig. 3(a) shows the phase diagram for $\phi = 0$]. Nevertheless, it can be shown [by comparing with the approximate boundaries obtained by perturbation theory in Δ_D, lines in Fig. 3(a)] that for low U the ground state is always $(S_z, T_z) = (0, 0)$ with a small region

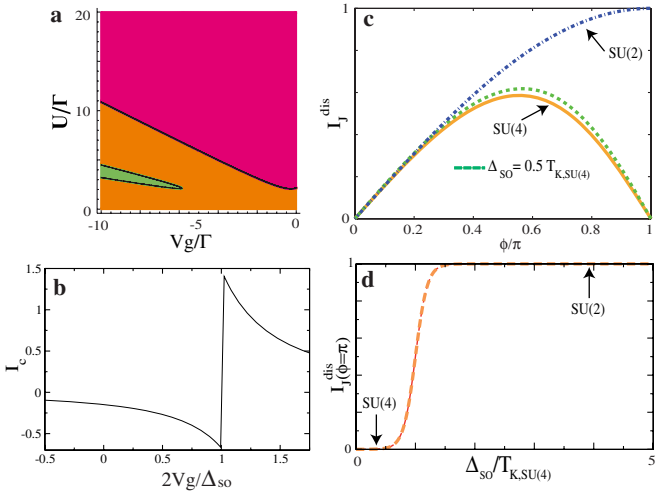

FIG. 3 (color online). Including charging effects at $B_{\|} = 0$. (a) Phase diagram in the large gap limit and $\phi = 0$. For large enough U, the ground state is $(S_z, T_z) = (\pm 1/2, \mp 1/2)$, dark gray (pink) region. For low U, the ground state is always $(S_z, T_z) = (0, 0)$, intermediate gray (orange), with a small region $(S_z, T_z) = (\pm 1/2, \pm 1/2)$, light gray (green). (b) Critical current versus gate voltage in the cotunneling limit. The critical current undergoes a 0-π transition when $V_g - \Delta_{SO}/2 = 0$. (c) Discrete Josephson current (in units of $\frac{e\Delta}{\hbar}$) versus ϕ in the Kondo limit. (d) Discrete Josephson current for $\phi = \pi$ versus SO coupling. As the system changes from SU(4) to SU(2) Kondo symmetries, I_J^{dis} goes from zero to maximum.

$(S_z, T_z) = (\pm 1/2, \pm 1/2)$. For large U, the ground state is always $(S_z, T_z) = (\pm 1/2, \mp 1/2)$ with energy $E_{GS}(\phi) = 2V_g - 1/2[\sqrt{4\Gamma^2 \cos^2(\phi/2) + (\Delta_{SO} + 2V_g + 3U)^2} + 3U]$. While we cannot identify this state with a π phase, it is likely that the inclusion of quantum fluctuations, by considering a finite gap, will stabilize the system towards this phase. Indeed, cotunneling corrections (for $\Gamma \ll \Delta$) present π phases. This can be shown by employing second-order perturbation theory in Γ [16,23]. In this limit, we find a supercurrent $I_J = I_c \sin(\phi)$ such that the overall sign of I_c governs the 0 or π character. In particular, the 0-π transition takes place at gate voltages corresponding to the resonant condition $V_g - \Delta_{SO}/2 = E_F = 0$, with a π phase for $V_g < \Delta_{SO}/2$, such that the transition can be tuned by V_g. Numerical results are shown in Fig. 3(b).

Beyond cotunneling, higher order tunneling events lead to Kondo physics. Here, we consider the large-U limit where simultaneous fluctuations in the spin and orbital quantum numbers lead to a highly symmetric SU(4) Kondo effect (for a Kondo temperature $T_{K,SU(4)} \gg \Delta$). When $T_{K,SU(4)} \gg \Delta_{SO}$, we find [16]

$$I_J^{dis} = \frac{e\Delta}{2\hbar} \sum_{\eta=\pm} \frac{\sin(\phi)}{[(1+\eta\alpha)^2 + 1][(1+\eta\alpha)^2 + \cos^2(\frac{\phi}{2})]}, \quad (3)$$

with $\alpha = \frac{\Delta_{SO}}{2T_{K,SU(4)}}$. When $T_{K,SU(4)} \ll \Delta_{SO}$, only the lower dot level participates in producing an SU(2) Kondo state. In the limit $T_{K,SU(2)} \gg \Delta$, the ABS are simply $E_1 = \pm\Delta\cos(\phi/2)$, namely, the ABS of a single contact with unitary transmission. The corresponding supercurrent is $I_J^{dis} = \frac{e\Delta}{\hbar}\sin(\phi/2)$, with $|\phi| < \pi$ [24]. Figure 3(c) summarizes these results. For both symmetries, the Josephson current always exhibits a 0-junction behavior, but the magnitude strongly depends on Δ_{SO}, as shown in Fig. 3(d). For $\Delta_{SO} = 0$, we recover the results of Ref. [25].

Our predictions are relevant in view of recent experimental advances in transport through ultraclean NTs with SO coupling [1]. Furthermore, most of the physics discussed here is inherent to the rich behavior that ABS show in the presence of SO coupling. We therefore expect that tunneling spectroscopy of individual ABS, like in the experiments of Ref. [21], may also reveal the effects described here. Microwave spectroscopy of excited ABS [26] is one further experimental example where our findings may be tested.

We thank Mahn-Soo Choi for his help at the initial stage of this project. R. A. is grateful to Leo Kouwenhoven for inspiring discussions. R. A. and R. L. were supported by MICINN Spain (Grants No. FIS2009-08744 and No. FIS2008-00781).

[1] F. Kuemmeth, S. Ilani, D. C. Ralph, and P. L. McEuen, Nature (London) **452**, 448 (2008).
[2] A. Y. Kasumov, R. Deblock, M. Kociak, B. Reulet, H. Bouchiat, I. I. Khodos, Y. B. Gorbatov, V. T. Volkov, C. Journet, and M. Burghard, Science **284**, 1508 (1999).
[3] A. F. Morpurgo, J. Kong, C. M. Marcus, and H. Dai, Science **286**, 263 (1999).
[4] P. Jarillo-Herrero, J. A. Van Dam, and L. P. Kouwenhoven, Nature (London) **439**, 953 (2006).
[5] J.-P. Cleziou, W. Wersnsdorfer, V. Bouchiat, T. Ondarcuhu, and M. Monthioux, Nature Nanotech. **1**, 53 (2006).
[6] For a review, see S. De Franceschi, L. P. Kouwenhoven, C. Schonenberger, and W. Wersndorfer, Nature Nanotech. **5**, 703 (2010).
[7] W. Liang, M. Bockrath, and H. Park, Phys. Rev. Lett. **88**, 126801 (2002).
[8] D. Cobden and J. Nygård, Phys. Rev. Lett. **89**, 046803 (2002).
[9] P. Jarillo-Herrero, J. Kong, H. S. J. van der Zant, C. Dekker, L. P. Kouwenhoven, and S. De Franceschi, Nature (London) **434**, 484 (2005).
[10] M.-S. Choi, R. López, and R. Aguado, Phys. Rev. Lett. **95**, 067204 (2005).
[11] E. Minot, Y. Yaish, and V. S. P. L. McEuen, Nature (London) **428**, 536 (2004).
[12] P. Jarillo-Herrero, J. Kong, H. S. J. van der Zant, C. Dekker, L. P. Kouwenhoven, and S. De Franceschi, Phys. Rev. Lett. **94**, 156802 (2005).

[13] Various band-structure calculations have been devoted to improve the first calculation in T. Ando, J. Phys. Soc. Jpn. **69**, 1757 (2000); see, e.g., D. Huertas-Hernando, F. Guinea, and A. Brataas, Phys. Rev. B **74**, 155426 (2006); L. Chico, M. P. Lopez-Sancho, and M. C. Munoz, Phys. Rev. B **79**, 235423 (2009); J. Jeong and H. Lee, Phys. Rev. B **80**, 075409 (2009); W. Izumida, K. Sato, and R. Saito, J. Phys. Soc. Jpn. **78**, 074707 (2009).

[14] T. Jespersen, K. Grove-Rasmussen, J. Paaske, K. Muraki, T. Fujisawa, J. Nygård, and K. Flensberg, Nature Phys. **7**, 348 (2011).

[15] We do not include effects originated from the finite length of the NT, such as the appearance of localized states near the boundaries of the NT. Transport can be fully suppressed at finite magnetic fields [M. del Valle, M. Margańska, and M. Grifoni, Phys. Rev. B **84**, 165427 (2011)] owing to these states, so we expect that they do not contribute to the Josephson effect described here.

[16] See Supplemental Material at http://link.aps.org/supplemental/10.1103/PhysRevLett.107.196801 for full details of the calculations.

[17] For realistic NT parameters, it is possible to obtain this effect without killing superconductivity: The field needed to induce the π-junction effect is $B_c \sim 0.5$ T, while ultraclean carbon nanotubes coupled to rhenium superconducting contacts can support supercurrents up to $\sim$1.5 T [Leo Kouwenhoven (private communication)].

[18] B. I. Spivak and S. A. Kivelson, Phys. Rev. B **43**, 3740 (1991).

[19] G. Tkachov and K. Richter, Phys. Rev. B **75**, 134517 (2007).

[20] E. Vecino, A. Martin-Rodero, and A. Levy Yeyati, Phys. Rev. B **68**, 035105 (2003).

[21] J.-D. Pillet, C. H. L. Quay, P. Morfin, C. Bena, A. Levy Yeyati, and P. Joyez, Nature Phys. **6**, 965 (2010).

[22] This has to be contrasted with magnetic π junctions which exhibit spontaneous supercurrents in frustrated loops and arrays at zero field; see S. M. Frolov, M. J. A. Stoutimore, T. A. Crane, D. J. Van Harlingen, V. A. Oboznov, V. V. Ryazanov, A. Ruosi, C. Granata, and M. Russo, Nature Phys. **4**, 32 (2007).

[23] T. Novotný, A. Rossini, and K. Flensberg, Phys. Rev. B **72**, 224502 (2005).

[24] C. W. J. Beenakker and H. van Houten, Phys. Rev. Lett. **66**, 3056 (1991).

[25] A. Zazunov, A. L. Yeyati, and R. Egger, Phys. Rev. B **81**, 012502 (2010).

[26] F. S. Bergeret, P. Virtanen, T. T. Heikkilä, and J. C. Cuevas, Phys. Rev. Lett. **105**, 117001 (2010).